Pramana – J. Phys. (2021) 95:150
https://doi.org/10.1007/s12043-021-02176-z

Novel formula for decay half-life of charged particle from the resonance of δ-well decorated Coulomb barrier

BASUDEB SAHU

Department of Physics, North Orissa University, Takatpur, Baripda 757 003, India
E-mail: bd_sahu@yahoo.com

MS received 29 March 2021; accepted 26 April 2021

Abstract. A nucleus, initially in a bound state akin to a Dirac δ well potential, under severe action of reflection from a repulsive electrostatic interaction at very small separation between the newly born α cluster and the daughter nucleus goes to the quasistationary state from which the decay of α sets in. The energy derivative of the phase-shift of the S-matrix of transition scattering from an isolated quasibound state to a scattering state is related to the width (Γ) of the resonance and hence the half-life $T_{1/2} = \ln 2\hbar/\Gamma$ of α-decay. Using exact solutions of the delta well driven Coulomb potential, we derive a compact expression for $\log_{10} T_{1/2}$ in terms of Q-value and the mass and charge numbers of the α emitter with a radius parameter specifying the sum of the charge radii of α and daughter nuclei or the radius of the parent emitter. The computed results of half-lives successfully explain the experimental values of α-decay half-lives ranging from 10^{-7}s to 10^{25}s in many light, heavy and superheavy radioactive nuclei with charge number $Z = 52$–120 and mass number $A = 106$–299. Showing uniformity in the applications of formulation to the decay of positive ions, namely α and cluster ions, the universal nature of the decay rule is established.

Keywords. Resonance scattering; phase-shift time; alpha decay; cluster emission; decay half-life.

PACS Nos **23.60.+e; 21.10.Tg; 23.70.+j; 27.90.+b**

1. Introduction

Akin to the process of emission of proton from nuclei beyond proton drip line [1], in the radioactivity of α emitters, the parent nucleus, ${}^{A+4}_{Z+2}X$, is unstable to the α decay:

$$ {}^{A+4}_{Z+2}X \rightarrow {}^{A}_{Z}X + \alpha. \tag{1}$$

Initially, the parent nucleus is in a bound state. Under the reflective action of the repulsive electrostatic interaction at very small separation between the newly born α cluster and the daughter nucleus, the parent nucleus goes to unbound or quasistationary state. It is from this quasistationary or resonance state that the decay of α cluster begins to occur with a positive energy of emission called Q-value. The ground-state α emission can be considered as one specific reaction channel (1) that characterised by the transition amplitude $T_{A+4,Z+2;A,Z}$.

The resonance width can be expressed through the transition amplitude [2,3] as

$$\Gamma = 2\pi |T_{A+4,Z+2;A,Z}|^2, \tag{2}$$

where the transition amplitude in the distorted-wave Born Approximation (DWBA) [1,2,4,5] is given by

$$T_{A+4,Z+2;A,Z} = \langle \phi_{A\alpha} \Psi_{A\alpha} | V_{A\alpha} | \Psi_{A+4} \rangle. \tag{3}$$

In eq. (3), $\phi_{A\alpha}$ is the incoming spherical wave representing the relative motion of the α-particle with respect to the daughter nucleus, $\Psi_{A\alpha}$ is the product of intrinsic wave functions of the α and the daughter nucleus, Ψ_{A+4} is the metastable state of the parent nucleus and $V_{A\alpha}$ is the interaction between the α and the daughter nucleus.

We, in this paper, shall approximate the true interaction $V_{A\alpha}$ with the much simpler one-body potential (see figure 1)

$$V(r) = V_N(r) + V_C(r), \tag{4}$$

where V_N(r) stands for the short-ranged attractive nuclear potential energy which is represented by a Dirac delta well:

$$V_N(r) = g\delta(r - R), \tag{5}$$

where g is a negative quantity and R denotes the physical range of the potential. $V_C(r)$ is the point charge repulsive

Published online: 03 September 2021

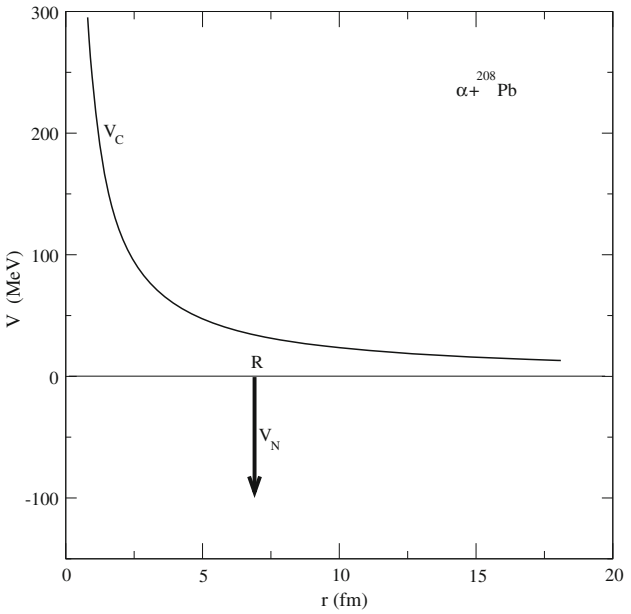

Figure 1. Schematic representation of the total potential energy (4) for an ion–ion system.

Coulomb potential energy expressed by

$$V_C(r) = \frac{Z_1 Z_2 e^2}{r}. \tag{6}$$

Here, numerically $e^2 = 1.4398$ MeV fm and Z_1 and Z_2 are the charge number of the two ions, α cluster and daughter nucleus. The above approximation of the true ion–ion interaction with a δ well plus Coulomb barrier is envisaged to implement the basic quantal result that the presence of a reflecting barrier potential entails a destabilisation of the bound state of the Dirac δ potential well and can even suppress it and generate unbound or resonance (quasistationary) state with positive energy eigenvalue [6].

The resonances generated by the total potential (4) are determined through the calculation of phase-shift of the S-matrix. According to a basic theorem [7], the energy derivative of the phase-shift, $2\mathrm{d}\theta/\mathrm{d}E$, is the time delay of the scattered wave packet which occurs due to the trapping of resonant state at that energy. So, at resonances, the phase-shift θ should rise sharply, that is, $\mathrm{d}\theta/\mathrm{d}E$ attains a maximum at the resonance energy $E = E_r$. For well-defined resonances, θ should pass through $\pi/2$ or more generally $(n + \frac{1}{2})\pi$ when n is an integer. Thus, in the variation of the quantity $\mathrm{d}\theta/\mathrm{d}E$ with energy E, the location of the maximum gives the resonant energy $E = E_r$ and the maximum value of $\mathrm{d}\theta/\mathrm{d}E$ calculated at $E = E_r$ gives the width Γ [7] as

$$\Gamma = 2\Big/\frac{\mathrm{d}\theta}{\mathrm{d}E}\Big|_{E=E_r} \tag{7}$$

and hence the decay half-life

$$T_{1/2} = 0.693\frac{\hbar}{2}\frac{\mathrm{d}\theta}{\mathrm{d}E}\Big|_{E=E_r}, \tag{8}$$

of the resonance state governing the decay process.

Using exact solutions of potential (4), we express the scattering phase-shift analytically and using the above property of phase-shift at resonance, we derive expressions for the width and hence the decay half-life $T_{1/2}$ in terms of incident energy and the sharp radius of the emitter of α cluster. The expression of $T_{1/2}$ when presented in the form of decimal logarithm of $T_{1/2}$ reduces to a simple formulae that can be used at ease to estimate the decay rate.

The formulation is equally applicable to the decay of positive ions, namely α and cluster of nucleons, with any charge number Z.

In §2, the details of formulation and derivation of the expressions for decay width and half-lives are given. Section 3 discusses the applications of formulation to explain the experimental data. In §4, we record the conclusion of the work.

2. Formulation

The δ-shell potential plus the Coulomb interaction is well understood and can be solved analytically [8–11]. Here, we briefly summarise some of the relevant results. The Hamiltonian is

$$H = H_0 + V_N(r). \tag{9}$$

The stronger interaction potential is V_N(r) and the free Hamiltonian H_0 consists of kinetic energy and Coulomb interaction

$$H_0 = -\frac{\hbar^2}{2\mu}\nabla^2 + V_C(r). \tag{10}$$

Here, μ denotes the reduced mass of the two-ion system with mass number A_1 and A_2, Coulomb potential $V_C(r)$ is given by (6). The δ-shell potential $V_N(r)$ is given by (5). We work in the centre-of-mass system and employ spherical coordinates. The radial wave function $\Psi_\ell(r) = u_\ell/r$ must be continuous at $r = R$, and its derivative $\mathrm{d}u_\ell/\mathrm{d}r$ fulfills

$$\frac{\mathrm{d}u_\ell(R^+)}{\mathrm{d}r} - \frac{\mathrm{d}u_\ell(R^-)}{\mathrm{d}r} = g u_\ell(R). \tag{11}$$

The radii R^+ and R^- are infinitesimally larger and smaller than R, respectively.

For positive energy $E = \hbar^2 k^2/2\mu$ we make the ansatz

$$u_\ell(r) = \begin{cases} iF_\ell(\eta, kr), & \text{if } r < R, \\ H^{(-)} - SH^{(+)}, & \text{if } r \geq R, \end{cases}$$

$$H^{(+)} = G_\ell(\eta, kr) + iF_\ell(\eta, kr),$$
$$H^{(-)} = G_\ell(\eta, kr) - iF_\ell(\eta, kr). \tag{12}$$

Here, $F_\ell(\eta, kr)$ in short F_ℓ and $G_\ell(\eta, kr)$ in short G_ℓ are the regular and irregular Coulomb wave functions, respectively and $S = e^{i\theta}$ stands for the scattering matrix with phase-shift θ. The Sommerfeld parameter $\eta = k_c/k$ where $k_c = Z_1Z_2e^2\mu/\hbar^2$ is the Coulomb momentum. Using matching condition (11) we get

$$S = \exp(i\theta) = \frac{1}{2}\left(G'_\ell F_\ell - F'_\ell G_\ell - \frac{g}{k}F_\ell G_\ell\right) + i\frac{g}{2k}F_\ell^2. \tag{13}$$

Here prime ($'$) indicates derivative with respect to $\rho = kr$. With the Wronskian $F'_\ell G_\ell - F_\ell G'_\ell = 1$, eq. (13) gives

$$\cot\theta = -\frac{1 + gF_\ell G_\ell/k}{(g/k)F_\ell^2}. \tag{14}$$

For the manifestation of resonance with positive eigenvalue E we set $\theta = \pi/2$ in (14) and find

$$g = -\frac{k}{F_\ell G_\ell}, \tag{15}$$

$$\frac{d\theta}{dk} = -\frac{1}{gF_\ell^2}\left(F_\ell\tilde{G}_\ell + G_\ell\tilde{F}_\ell - \frac{F_\ell G_\ell}{k}\right)\frac{k}{F_\ell G_\ell}, \tag{16}$$

where the symbol, $\tilde{}$, indicates derivative with respect to k. Using the result of g (15) in (16) we get

$$\frac{d\theta}{dk} = \frac{F_\ell\tilde{G}_\ell + G_\ell\tilde{F}_\ell - F_\ell G_\ell/k}{F_\ell^2}. \tag{17}$$

With the conversion

$$\frac{d\theta}{dk} = \frac{\hbar^2 k}{\mu}\frac{d\theta}{dE}$$

and the result of eq. (7), expression (17) yields

$$\frac{E_r}{\Gamma} = \frac{k(F_\ell\tilde{G}_\ell + G_\ell\tilde{F}_\ell) - F_\ell G_\ell}{4F_\ell^2}. \tag{18}$$

The Coulomb wave functions have been expanded into a series of modified Bessel functions in ref. [11] whose coefficients decrease with inverse power of η. With $\eta = k_c/k$ and $\rho = kR$, these functions for s-wave are given by

$$F_0(\eta, \rho) = \frac{C_0(\eta)}{2\eta}\sum_{n=1}^{\infty} b_n(2k_cR)^{n/2}I_n(2\sqrt{2k_cR}), \tag{19}$$

$$G_0(\eta, \rho) = \frac{2}{\beta_0(\eta)C_0(\eta)} \times \sum_{n=1}^{\infty}(-1)^n b_n(2k_cR)^{n/2}K_n(2\sqrt{2k_cR}). \tag{20}$$

Here,

$$b_1 = 1$$
$$b_2 = 0$$
$$b_3 = -\frac{1}{4\eta^2}$$
$$b_4 = -\frac{1}{12\eta^2}. \tag{21}$$

We have for $\eta \gg 1$ [12]

$$C_0(\eta) = \sqrt{2\pi\eta}e^{-\pi\eta}, \tag{22}$$

$$\beta_0(\eta) = -1 + \mathcal{O}(\eta^{-4}). \tag{23}$$

We also have the modified Bessel functions as [12]

$$I_n(z) \approx \frac{e^z}{\sqrt{2\pi z}}\left[1 - \frac{4\nu^2 - 1}{8z}\right], \tag{24}$$

$$K_n(z) \approx \sqrt{\frac{\pi}{2z}}e^{-z}\left[1 + \frac{4\nu^2 - 1}{8z}\right], \tag{25}$$

valid for $z \to \infty$ with $\nu = 1, 2, 3, \ldots$.

Using the results of eqs (24) and (25) in eqs (19) and (20), we express $F_0(\eta, \rho)$ and $G_0(\eta, \rho)$ in leading orders of term $\eta \gg 1$. With the specification $z = 2\sqrt{2k_cR}$,

$$F_0 = \frac{C_0}{2\eta}\left[(2k_cR)^{1/2}I_1(z) - \frac{1}{4\eta^2}(2k_cR)^{3/2}I_3(z) - \frac{1}{12\eta^2}(2k_cR)^2 I_4(z)\right], \tag{26}$$

$$G_0 = \frac{2}{C_0}(2k_cR)^{1/2}K_1(z) - \frac{1}{2\eta^2C_0}(2k_cR)^{3/2}K_3(z) + \frac{1}{6\eta^2C_0}(2k_cR)^2K_4(z). \tag{27}$$

Here, C_0 is given by (22). Using these results of F_0 and G_0 and their derivatives with respect to k, and neglecting $1/\eta^5$ terms in these expansions, one can simplify expression (18) for s-wave to give [11]

$$\frac{E_r}{\Gamma} = \left(\frac{kR}{3C_0^2}\right)\frac{\sqrt{2k_cR}(I_1K_4 - I_4K_1) - 3(I_1K_3 + I_3K_1)}{I_1^2}. \tag{28}$$

Using the results of eqs (24) and (25), expression (28) can further be simplified to yield in leading order of term $z = 2\sqrt{2k_cR} \gg 1$

$$\frac{\Gamma}{E_r} = \left(\frac{6}{7}\right)\frac{4k_c}{k^2R}e^{4\sqrt{2k_cR}}e^{-2\pi\eta}. \tag{29}$$

It may be pointed out that eq. (29) is the same as (A25) given in [11] with the approximation $(6/7) \approx 1$. With $E_r = \hbar^2k^2/2\mu$ and $k_c = Z_1Z_2e^2\mu/\hbar^2$, eq. (29) reduces to

$$\Gamma = \frac{12Z_1Z_2e^2}{7R}\exp(4\sqrt{2k_cR} - 2\pi\eta). \tag{30}$$

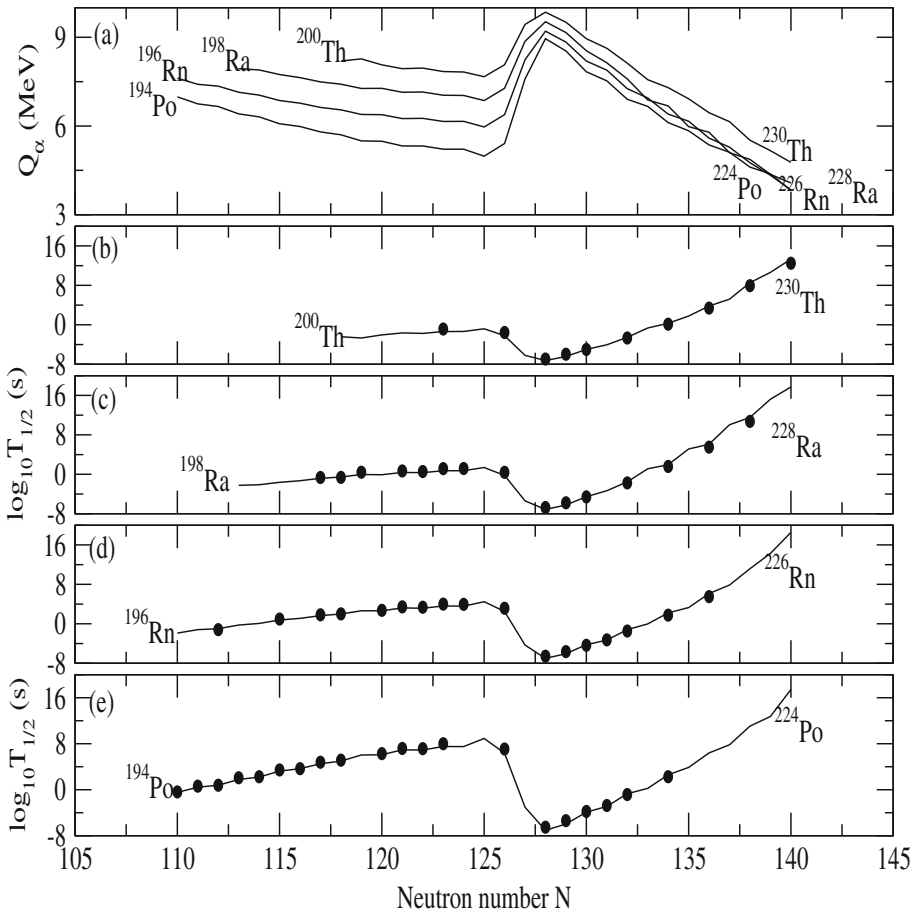

Figure 2. (**a**) Plot of α-decay energy, Q_α, obtained from [14], as a function of the neutron number N of the parent nucleus for the isotopes of Th, Ra, Rn and Po elements, (**b**) plot of decimal logarithm of half-life, $\log_{10} T_{1/2}$, as a function of the neutron number N of the parent nucleus for the isotopes of the Th element. The calculated results obtained by using formulae (32) are shown by a full curve. The solid circles represent experimental values obtained from ref. [15], (**c**) same as figure 2b for the Ra element, (**d**) same as figure 2b for the Rn element and (**e**) same as figure 2b for the Po element.

The corresponding decay half-life $T_{1/2} = \ln 2\hbar/\Gamma$ is expressed as

$$T_{1/2} = \left(\frac{7}{12}\right)\frac{0.693\hbar R}{Z_1 Z_2 e^2}\exp(2\pi\eta - 4\sqrt{2k_c R}). \tag{31}$$

The decimal logarithm of $T_{1/2}$ (31) is given in sec by

$$\log_{10} T_{1/2} = a\chi + b\zeta + c + h_{\log}. \tag{32}$$

Here

$$\chi = Z_1 Z_2\left(\frac{A_1 A_2}{(A_1 + A_2)E_r}\right)^{1/2}, \tag{33}$$

$$\zeta = \left(\frac{Z_1 Z_2 A_1 A_2 R}{A_1 + A_2}\right)^{1/2}, \tag{34}$$

$$h_{\log} = \log_{10}\left(\frac{R}{Z_1 Z_2}\right), \tag{35}$$

$$a = \pi(0.4342944819)(1.4398)\frac{\sqrt{2\times 931.5}}{197.329} = 0.42968, \tag{36}$$

$$b = -4(0.4342944819)\frac{\sqrt{2\times 931.5\times 1.4398}}{197.329} = -0.45594, \tag{37}$$

$$c = \log_{10}\left(\frac{0.693\times 197.5\times 7}{36\times 1.4398}\right) - 23 = -21.73320. \tag{38}$$

Here, the physical range R of the delta well can be related to the sum of the charge radii [11] of the emitted particle and the daughter nucleus with mass numbers A_1 and A_2, respectively, as

$$R = r_c(A_1^{1/3} + A_2^{1/3}), \tag{39}$$

with $r_c \approx 1.0$ fm. Alternately, one can consider this parameter R as the sharp radius [13] of the parent nucleus with combined mass, $A_1 + A_2$, as

$$R = 1.28(A_1 + A_2)^{1/3} + 0.8(A_1 + A_2)^{-1/3} - 0.76. \tag{40}$$

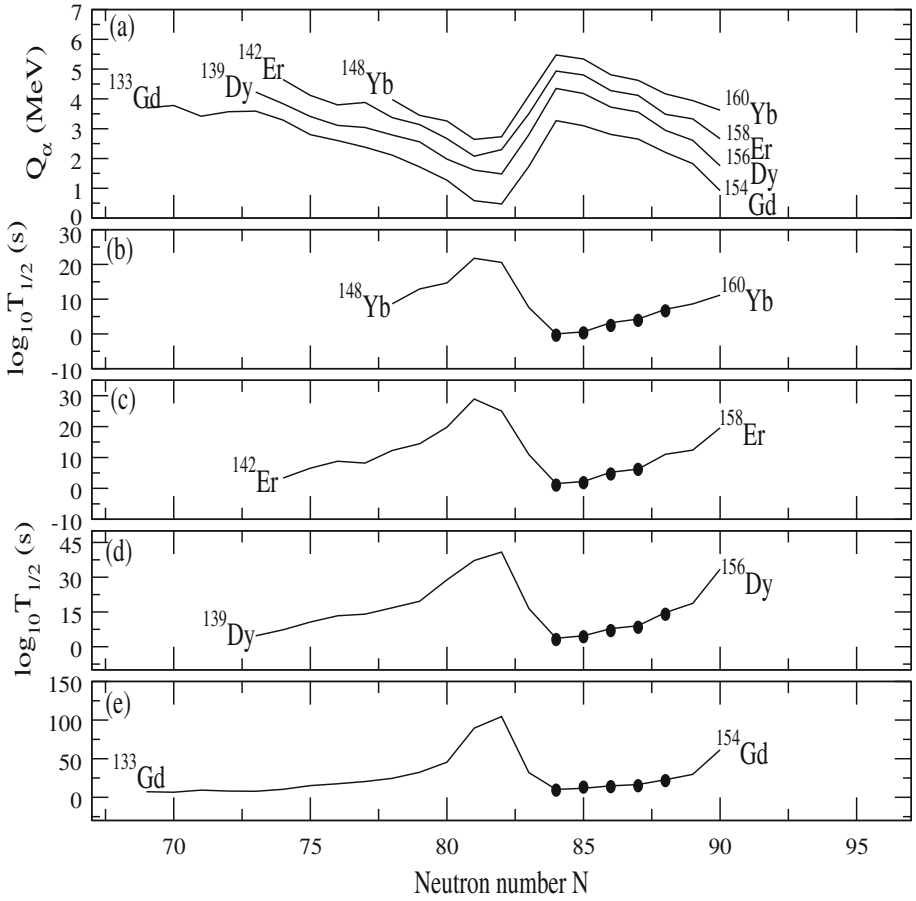

Figure 3. (**a**) Same as figure 2a for the Yb, Er, Dy and Gd elements, (**b**) same as figure 2b for the Yb element, (**c**) same as figure 2b for the Er element, (**d**) same as figure 2b for the Dy element and (**e**) same as figure 2b for the Gd element.

It is striking to note that formulae (32) does not depend on the potential parameter g except the physical range R of the δ well which, in term, is related to the sum of the charge radii (39) of the emitted particle and daughter nucleus or the size of the emitter (parent) nucleus by (40). Hence, one can take (32) as a parameter-free formulae and predict result of half-life of decay of positive ion from the emitter depending on the characteristic energy of emission $E_r = Q$-value in MeV and mass and charge numbers of the emitted ion and the daughter nucleus available in mass tables in the literature. Further, in a specific decay event, one can fit the measured value of decay rate closely by varying the charge radius parameter r_c of (39) in the computation of eq. (32) and understand the physically observed results of charge radii of the participants of the event as done in the cases of $\alpha + \alpha$, proton$+^{16}$O resonances [11].

In the next section we apply the formulation to explain the experimental data of decay half-lives in α as well as cluster decay events.

3. Numerical results and discussion

For a nucleus undergoing α emission, the emission energy or Q_α value is obtained from the atomic mass table [14]. Using this Q_α in MeV as E_r and the value of the radius parameter R (40) decided by mass and charge numbers of the emitter, we compute formula (32) for the result of decimal logarithm of decay half-life $\log_{10} T_{1/2}$. This calculated result is denoted by $\log_{10} T_{1/2}^{\text{form}}$ and is compared with the corresponding experimental result, $\log_{10} T_{1/2}^{\text{expt}}$. Q_α obtained from the mass table [14] of different nuclei in the series of isotopes of Po, Rn, Ra and Th elements are shown in figure 2a. We compare our results of $\log_{10} T_{1/2}^{\text{form}}$ shown by solid curve with the results of $\log_{10} T_{1/2}^{\text{expt}}$ (solid circle) obtained from [15] for the isotopes of elements Th in figure 2b, Ra in figure 2c, Rn in figure 2d and Po in figure 2e. It is seen that the comparison between the calculated (solid curve) and the experimental (solid circle) is good in each of the

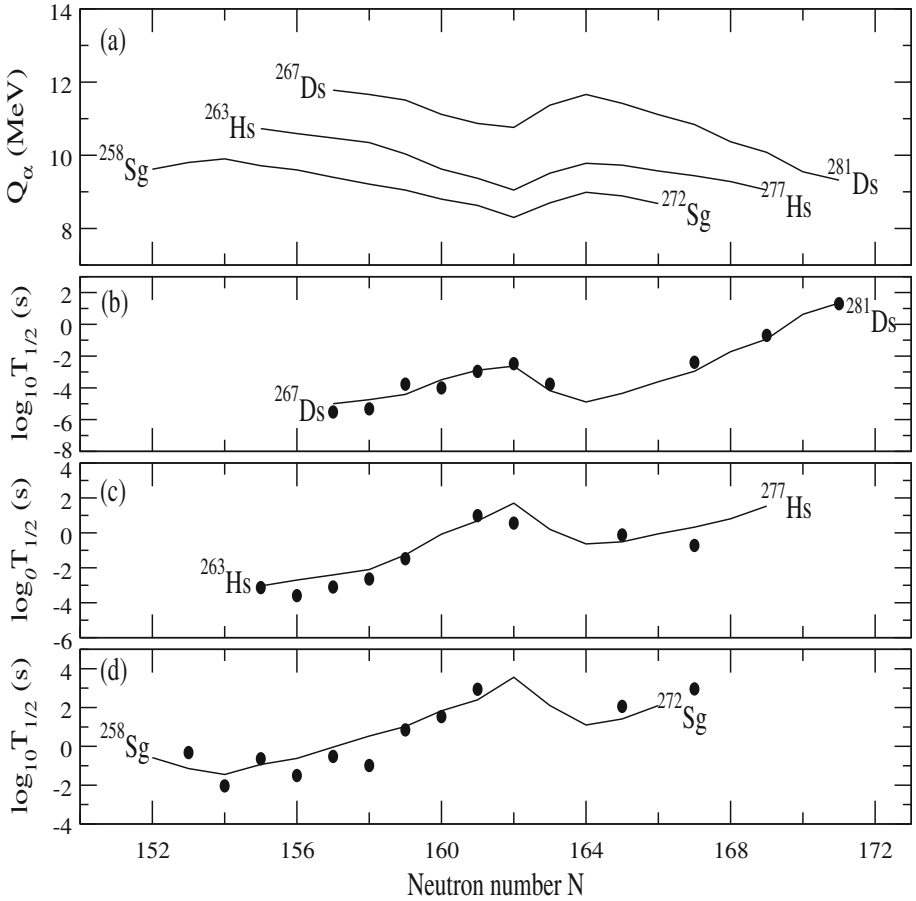

Figure 4. (**a**) Same as figure 2a for the Ds, Hs and Sg elements, (**b**) same as figure 2b for the Ds element, (**c**) same as figure 2b for the Hs element and (**d**) same as figure 2b for the Sg element.

four groups of isotopes stated above. Further, the nice explanation of the measured results is extended to the neutron-deficient regions in each of these cases equally well.

In figure 3, we compare our calculated results of $\log_{10} T^{\text{form}}_{1/2}$ (solid curve) with the corresponding experimental data $\log_{10} T^{\text{expt}}_{1/2}$ (solid circle) [15] for the isotopes of light α emitters, namely Gd, Dy, Er and Yb. The available data [15] in the neutron-rich region are successfully explained in these cases. We have extended the calculation of $T_{1/2}$ to the neutron-deficient regions and these results (solid curve) can be referred in future measurements of α decay half-lives in these cases of light α emitters.

In figure 4, we give a successful explanation of the experimental results of $T^{\text{expt}}_{1/2}$ [15] in the form $\log_{10} T^{\text{expt}}_{1/2}$ as a function of N for the isotopes of heavy elements, namely Sg, Hs and Ds by our calculated results of $\log_{10} T^{\text{form}}_{1/2}$ shown by solid curves.

In order to understand the physical content of the range parameter R (39), we wish to fit the experimental values of α-decay half-lives of several nuclei with different measured Q_α values individually by varying the values of R or r_c (39). The measured results of Q_α and half-lives of 390 nuclei consisting of elements with $Z = 52$–120 and $A = 106$–299 are obtained from ref. [15]. Using this value of Q_α in formula (32), the value of r_c is varied to get the calculated result of half-life $T^{\text{form}}_{1/2}$ close to the experimental value $T^{\text{expt}}_{1/2}$ such that the deviation $D\ (= |\log_{10} T^{\text{expt}}_{1/2} - \log_{10} T^{\text{form}}_{1/2}|) \leq 0.0022$. This closeness in fitting the data of α-decay half-lives of 390 nuclei is depicted in figure 5 and the corresponding values of r_c used in these calculations for different nuclei are presented in figure 6. As seen in figure 6, the value of r_c does not vary much for different nuclei and is about 0.93 fm. This gives an important information about the sum of the charge radii as $R = r_c(A_\alpha^{1/3} + A_d^{1/3})$ with $r_c = 0.93$ fm of the two ions involved in the decay of the parent nucleus from the resonance state of the α+daughter nucleus system with mass numbers A_α and A_d, respectively. This finding is consistent with the result of the sum of the charge radii of α clusters

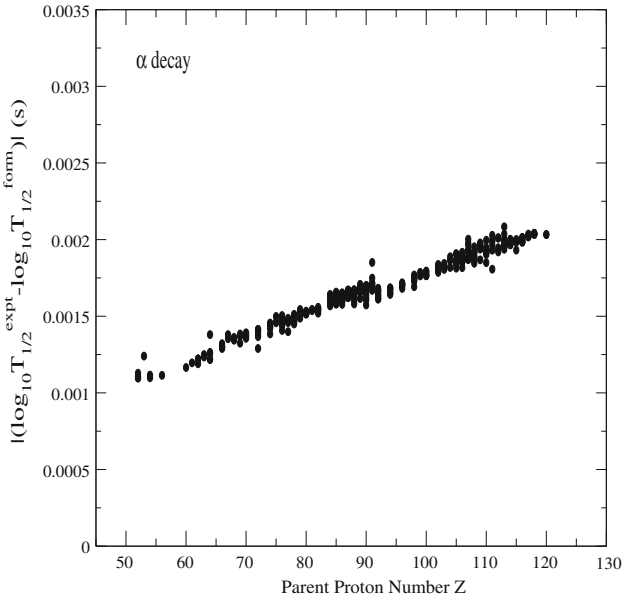

Figure 5. Deviation of the calculated values of the decimal logarithm of α-decay half-life using formulae (32) from the experimental ones for 390 nuclei in the range $Z = 52$–120 collected from ref. [15].

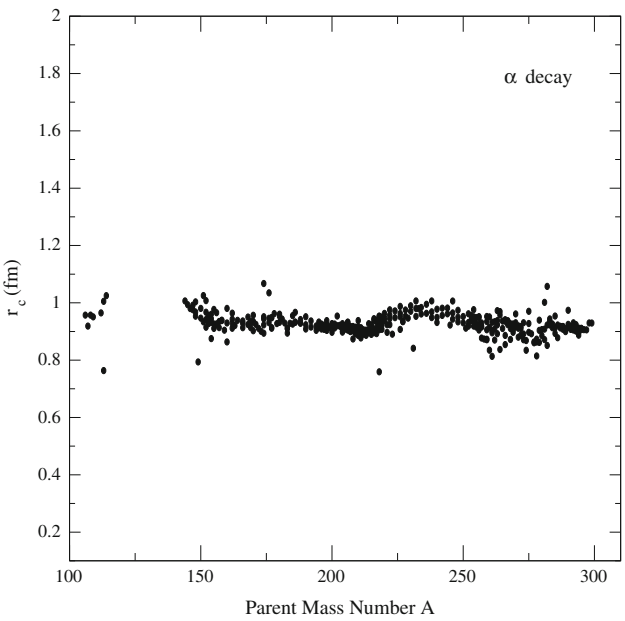

Figure 6. Plot of the range parameter r_c defined by eq. (39) as a function of atomic mass number A of 390 nuclei.

(≈ 3.3 fm) found from the $\alpha + \alpha$ resonance state of ^{8}Be nucleus [11].

We may compare our results of half-lives $T_{1/2}^{\text{form}}$ with the values of decay half-lives of a successful calculation, the universal decay law (UDL), developed by Qi *et al* [16]. This law is expressed by the following equation:

$$\log_{10} T_{1/2} = a' Z_c Z_d \sqrt{\frac{A_c A_d}{E(A_c + A_d)}} + b' \sqrt{\frac{A_c A_d Z_c Z_d}{(A_c + A_d)}(A_c^{1/3} + A_d^{1/3})} + c', \tag{41}$$

where Z_c and A_c are the charge and mass numbers of the emitted cluster which in this case is an α-particle. The constants $a' = 0.4065$, $b' = -0.4311$ and $c' = -20.7889$ are determined [16] by fitting to experimental data of α-decay half-lives of 139 nuclei with Z =78–118 obtained from ref. [17]. In table 1, we present these data of measured values of decay half-lives as $T_{1/2}^{\text{expt}}$ in the third column and the calculated values, $T_{1/2}^{\text{UDL}}$, given by (41) in the fifth column. In the fourth column of table 1, we record our results of half-lives, $T_{1/2}^{\text{form}}$, obtained by computing formula (31) by using a common radius parameter $r_c = 0.937$ fm for all 139 nuclei. On comparison with the results of $T_{1/2}^{\text{UDL}}$ we see in table 1 that our calculated values, $T_{1/2}^{\text{form}}$, are quite close to the respective $T_{1/2}^{\text{UDL}}$ values and they explain the corresponding experimental data, $T_{1/2}^{\text{expt}}$, in the third column quite well.

Here, we briefly evaluate our overall calculations. To measure the goodness of the agreement between the results of half-lives from the experiments and the present calculations, we obtain the deviation (D_i) of the values of $T_{1/2}^{\text{form}}$ calculated with a common value of $r_c = 0.937$ fm from the experimental data ($T_{1/2}^{\text{expt}}$) given by the relation

$$D_i = \left| \log_{10} T_{1/2}^{\text{form}} - \log_{10} T_{1/2}^{\text{expt}} \right|_i \tag{42}$$

for a given nucleus. The standard root mean square deviation (σ) of $\log_{10} T_{1/2}^{\text{form}}$ from $\log_{10} T_{1/2}^{\text{expt}}$ for n nuclei is defined as [20]

$$\sigma = \sqrt{\frac{1}{n-1} \sum_{i=1}^{n} D_i^2}. \tag{43}$$

The $T_{1/2}^{\text{UDL}}$ results given by (41) with the values of parameters $a' = 0.4065$, $b' = -0.4311$ and $c' = -20.7889$ for 139 nuclei listed in table 1 give standard deviation $\sigma = 0.343$ representing a factor of about 2.2 indicating good quality fitting of the data [16]. This result of fitting of the experimental data in UDL formulation is obtained by simultaneous variation of three parameters namely a', b' and c' in (41). By applying our formula (31) to the above 139 α emitters, we get $\sigma = 0.453$ corresponding to a factor of about 2.8 which is quite close to 2.2,

Table 1. Comparison of the experimental α-decay half-lives with the calculated ones for different isotopes of parent nuclei with $Z = 78$–118. The first column denotes the parent nuclei. The second and third columns are, respectively, the experimental decay energies Q_α^{expt} and half-lives $T_{1/2}^{\text{expt}}$ of α decay. The results of half-lives $T_{1/2}^{\text{form}}$ of the present formulation (31) obtained by using a fixed value for $r_c = 0.937$ fm are listed in the fourth column. Results of α-decay half-lives of UDL are given in the 5th column as $T_{1/2}^{\text{UDL}}$. Experimental data of α-decay half-lives and Q_α values are obtained from ref. [17].

Nuclei	Q_α^{expt} (MeV)	$T_{1/2}^{\text{expt}}$ (s)	$T_{1/2}^{\text{form}}$ (s)	$T_{1/2}^{\text{UDL}}$ (s)
^{166}Pt	7.286	3.0×10^{-4}	1.54×10^{-4}	3.78×10^{-4}
^{168}Pt	6.997	2.0×10^{-3}	1.33×10^{-3}	2.88×10^{-3}
^{170}Pt	6.708	1.4×10^{-2}	1.33×10^{-2}	2.53×10^{-2}
^{172}Pt	6.465	1.3×10^{-1}	1.02×10^{-1}	1.74×10^{-1}
^{174}Pt	6.184	1.2×10^{0}	1.29×10^{0}	1.90×10^{0}
^{176}Pt	5.885	1.7×10^{1}	2.38×10^{1}	2.97×10^{1}
^{178}Pt	5.573	2.7×10^{2}	6.43×10^{2}	6.66×10^{2}
^{180}Pt	5.240	1.7×10^{4}	3.03×10^{4}	2.53×10^{4}
^{182}Pt	4.952	3.5×10^{5}	1.15×10^{6}	7.88×10^{5}
^{172}Hg	7.525	4.2×10^{-4}	1.42×10^{-4}	3.42×10^{-4}
^{174}Hg	7.233	2.1×10^{-3}	1.19×10^{-3}	2.55×10^{-3}
^{176}Hg	6.897	2.3×10^{-2}	1.67×10^{-2}	3.08×10^{-2}
^{178}Hg	6.577	3.8×10^{-1}	2.49×10^{-1}	3.94×10^{-1}
^{180}Hg	6.258	5.3×10^{0}	4.56×10^{0}	6.12×10^{0}
^{182}Hg	5.997	7.8×10^{1}	5.77×10^{1}	6.72×10^{1}
^{184}Hg	5.662	2.8×10^{3}	2.00×10^{3}	1.91×10^{3}
^{186}Hg	5.205	5.2×10^{5}	4.56×10^{6}	3.23×10^{5}
^{188}Hg	4.705	5.3×10^{8}	4.29×10^{8}	2.09×10^{8}
^{178}Pb	7.790	2.3×10^{-4}	1.09×10^{-4}	2.61×10^{-4}
^{180}Pb	7.415	5.0×10^{-3}	1.63×10^{-3}	3.36×10^{-3}
^{182}Pb	7.066	5.5×10^{-2}	2.47×10^{-2}	4.36×10^{-2}
^{184}Pb	6.774	6.1×10^{-1}	2.78×10^{-1}	4.28×10^{-1}
^{186}Pb	6.470	1.2×10^{1}	4.16×10^{0}	5.50×10^{0}
^{188}Pb	6.109	2.7×10^{2}	1.37×10^{2}	1.49×10^{2}
^{190}Pb	5.697	1.8×10^{4}	1.13×10^{4}	9.70×10^{3}
^{192}Pb	5.221	3.6×10^{6}	3.63×10^{6}	2.25×10^{6}
^{194}Pb	4.738	9.8×10^{9}	3.06×10^{9}	1.31×10^{9}
^{210}Pb	3.792	3.7×10^{16}	3.73×10^{16}	6.35×10^{15}
^{188}Po	8.082	4.3×10^{-43}	5.84×10^{-5}	1.40×10^{-4}
^{190}Po	7.693	2.5×10^{-3}	8.97×10^{-4}	1.83×10^{-3}
^{192}Po	7.319	3.3×10^{-2}	1.52×10^{-2}	2.67×10^{-2}
^{194}Po	6.987	3.9×10^{-1}	2.26×10^{-1}	3.41×10^{-1}
^{196}Po	6.657	5.9×10^{0}	4.06×10^{0}	5.21×10^{0}
^{198}Po	6.309	1.9×10^{2}	1.10×10^{2}	1.17×10^{2}
^{200}Po	5.981	6.2×10^{3}	3.22×10^{3}	2.85×10^{3}
^{202}Po	5.701	1.4×10^{5}	7.18×10^{4}	5.34×10^{4}
^{204}Po	5.485	1.9×10^{6}	9.11×10^{5}	5.88×10^{5}
^{206}Po	5.327	1.4×10^{7}	6.32×10^{6}	3.65×10^{6}
^{208}Po	5.215	9.1×10^{7}	2.58×10^{7}	1.37×10^{7}
^{210}Po	5.407	1.2×10^{7}	1.91×10^{6}	1.16×10^{6}
^{212}Po	8.954	3.0×10^{-7}	7.30×10^{-8}	2.34×10^{-7}
^{214}Po	7.833	1.6×10^{-4}	1.13×10^{-4}	2.43×10^{-4}
^{216}Po	6.906	1.5×10^{-1}	1.82×10^{-1}	2.62×10^{-1}
^{218}Po	6.115	1.9×10^{2}	3.62×10^{2}	3.43×10^{2}
^{196}Rn	7.617	4.7×10^{-3}	8.75×10^{-3}	1.55×10^{-2}
^{198}Rn	7.349	6.5×10^{-2}	6.91×10^{-2}	1.09×10^{-1}
^{200}Rn	7.044	1.0×10^{0}	8.53×10^{-1}	1.17×10^{0}
^{202}Rn	6.774	1.2×10^{1}	9.04×10^{0}	1.08×10^{1}
^{204}Rn	6.545	1.1×10^{2}	7.44×10^{1}	7.95×10^{1}
^{206}Rn	6.384	5.5×10^{2}	3.43×10^{2}	3.35×10^{2}
^{208}Rn	6.261	2.4×10^{3}	1.12×10^{3}	1.02×10^{3}
^{210}Rn	6.159	9.0×10^{3}	3.07×10^{3}	2.63×10^{3}
^{212}Rn	6.385	1.4×10^{3}	2.64×10^{2}	2.58×10^{2}
^{214}Rn	9.208	2.7×10^{-7}	8.28×10^{-8}	2.62×10^{-7}
^{216}Rn	8.200	4.5×10^{-5}	4.95×10^{-5}	1.10×10^{-4}
^{218}Rn	7.262	3.5×10^{-2}	6.13×10^{-2}	9.25×10^{-2}
^{220}Rn	6.405	5.6×10^{1}	1.55×10^{2}	1.53×10^{2}
^{222}Rn	5.590	3.3×10^{5}	1.37×10^{6}	8.23×10^{5}
^{202}Ra	8.020	2.6×10^{-3}	2.17×10^{-3}	4.08×10^{-3}
^{204}Ra	7.636	5.9×10^{-2}	3.82×10^{-2}	6.12×10^{-2}
^{206}Ra	7.415	2.4×10^{-1}	2.12×10^{-1}	3.09×10^{-1}
^{208}Ra	7.273	1.4×10^{0}	6.50×10^{-1}	8.84×10^{-1}
^{210}Ra	7.152	3.8×10^{0}	1.71×10^{0}	2.19×10^{0}
^{212}Ra	7.032	1.4×10^{1}	4.59×10^{0}	5.55×10^{0}
^{214}Ra	7.273	2.5×10^{0}	5.04×10^{-1}	6.84×10^{-1}
^{216}Ra	9.526	1.8×10^{-7}	6.50×10^{-8}	2.06×10^{-7}
^{218}Ra	8.546	2.6×10^{-5}	2.65×10^{-5}	6.05×10^{-5}
^{220}Ra	7.592	1.8×10^{-2}	2.76×10^{-2}	4.32×10^{-2}
^{222}Ra	6.697	3.8×10^{1}	7.03×10^{1}	7.15×10^{1}
^{224}Ra	5.789	3.3×10^{5}	1.23×10^{6}	7.34×10^{5}
^{226}Ra	4.871	5.3×10^{10}	3.51×10^{11}	1.05×10^{11}
^{210}Th	8.053	1.7×10^{-2}	8.07×10^{-3}	1.37×10^{-2}
^{212}Th	7.952	3.6×10^{-2}	1.60×10^{-2}	2.61×10^{-2}
^{214}Th	7.826	1.0×10^{-1}	3.91×10^{-2}	6.07×10^{-2}
^{216}Th	8.071	2.7×10^{-2}	5.46×10^{-3}	9.36×10^{-2}
^{218}Th	9.849	1.1×10^{-07}	5.04×10^{-8}	1.60×10^{-7}
^{220}Th	8.953	9.7×10^{-6}	9.96×10^{-6}	2.37×10^{-5}
^{222}Th	8.127	2.0×10^{-3}	2.79×10^{-3}	4.88×10^{-3}
^{224}Th	7.298	1.0×10^{0}	2.07×10^{0}	2.52×10^{0}
^{226}Th	6.451	1.8×10^{3}	6.48×10^{3}	5.08×10^{3}
^{228}Th	5.520	6.0×10^{7}	3.63×10^{8}	1.57×10^{8}
^{230}Th	4.770	2.4×10^{12}	2.29×10^{13}	5.43×10^{12}
^{218}U	8.786	1.5×10^{-3}	1.93×10^{-4}	3.94×10^{-4}
^{220}U	1.03	6.0×10^{-8}	1.99×10^{-8}	6.61×10^{-8}
^{222}U	9.500	1.4×10^{-6}	1.70×10^{-6}	4.43×10^{-6}
^{224}U	8.620	7.0×10^{-4}	4.71×10^{-4}	8.98×10^{-4}
^{226}U	7.701	5.0×10^{-1}	4.62×10^{-1}	6.05×10^{-1}
^{228}U	6.803	8.0×10^{2}	1.45×10^{3}	1.22×10^{3}
^{230}U	5.993	2.7×10^{6}	9.43×10^{6}	4.92×10^{6}
^{232}U	5.414	3.2×10^{9}	1.60×10^{10}	5.57×10^{9}
^{234}U	4.858	7.7×10^{12}	6.91×10^{13}	1.52×10^{13}

Table 1. *Continued.*

Nuclei	Q_α^{expt} (MeV)	$T_{1/2}^{\text{expt}}$ (s)	$T_{1/2}^{\text{form}}$ (s)	$T_{1/2}^{\text{UDL}}$ (s)
^{236}U	4.573	7.4×10^{14}	8.74×10^{15}	1.47×10^{15}
^{228}Pu	7.950	2.0×10^{-1}	3.95×10^{-1}	5.16×10^{-1}
^{230}Pu	7.180	1.0×10^{2}	2.92×10^{2}	2.66×10^{2}
^{232}Pu	6.716	9.9×10^{3}	2.61×10^{4}	1.86×10^{4}
^{234}Pu	6.310	5.3×10^{5}	1.98×10^{6}	1.11×10^{6}
^{236}Pu	5.867	9.0×10^{7}	3.78×10^{8}	1.58×10^{8}
^{238}Pu	5.593	2.8×10^{9}	1.28×10^{10}	4.44×10^{9}
^{240}Pu	5.256	2.1×10^{11}	1.47×10^{12}	3.91×10^{11}
^{242}Pu	4.984	1.2×10^{13}	9.47×10^{13}	2.00×10^{13}
^{244}Pu	4.665	2.5×10^{15}	2.01×10^{16}	3.18×10^{15}
^{238}Cm	6.620	2.3×10^{5}	5.11×10^{5}	3.03×10^{5}
^{240}Cm	6.397	2.3×10^{6}	5.62×10^{6}	2.91×10^{6}
^{242}Cm	6.216	1.4×10^{7}	4.27×10^{7}	1.98×10^{7}
^{244}Cm	5.902	5.7×10^{8}	1.92×10^{9}	7.22×10^{8}
^{246}Cm	5.475	1.5×10^{11}	5.95×10^{11}	1.63×10^{11}
^{248}Cm	5.162	1.2×10^{13}	6.12×10^{13}	1.30×10^{13}
^{240}Cf	7.719	6.5×10^{1}	8.61×10^{1}	8.08×10^{1}
^{242}Cf	7.516	2.6×10^{2}	4.89×10^{2}	4.16×10^{2}
^{244}Cf	7.329	1.2×10^{3}	2.58×10^{3}	1.99×10^{3}
^{246}Cf	6.861	1.3×10^{5}	2.54×10^{5}	1.52×10^{5}
^{248}Cf	6.361	2.9×10^{7}	6.02×10^{7}	2.68×10^{7}
^{250}Cf	6.128	4.1×10^{8}	9.29×10^{8}	3.55×10^{8}
^{252}Cf	6.217	8.6×10^{7}	2.88×10^{8}	1.16×10^{8}
^{254}Cf	5.926	1.7×10^{9}	1.04×10^{10}	3.47×10^{9}
^{246}Fm	8.374	1.3×10^{0}	1.98×10^{0}	2.23×10^{0}
^{248}Fm	8.002	3.9×10^{1}	3.88×10^{1}	3.71×10^{1}
^{250}Fm	7.557	2.0×10^{3}	1.85×10^{3}	1.43×10^{3}
^{252}Fm	7.152	9.1×10^{4}	8.54×10^{4}	5.33×10^{4}
^{254}Fm	7.307	1.2×10^{4}	1.70×10^{4}	1.15×10^{4}
^{256}Fm	7.027	1.2×10^{5}	2.61×10^{5}	1.52×10^{5}
^{252}No	8.549	3.6×10^{0}	2.55×10^{0}	2.78×10^{0}
^{254}No	8.226	5.7×10^{1}	3.21×10^{1}	3.03×10^{1}
^{256}No	8.581	2.9×10^{0}	1.69×10^{0}	1.87×10^{0}
^{254}Rf	9.380	$>1.5 \times 10^{-3}$	3.07×10^{-2}	4.21×10^{-2}
^{256}Rf	8.930	2.0×10^{0}	7.35×10^{-1}	8.44×10^{-1}
^{258}Rf	9.250	9.2×10^{-2}	6.54×10^{-2}	8.52×10^{-2}
^{258}Sg	9.670	$>1.6 \times 10^{-2}$	2.01×10^{-2}	2.78×10^{-2}
^{260}Sg	9.920	7.2×10^{-3}	3.52×10^{-3}	5.31×10^{-3}
^{262}Sg	9.600	$>3.6 \times 10^{-2}$	2.77×10^{-2}	3.72×10^{-2}
^{266}Sg	8.880	2.6×10^{1}	4.46×10^{0}	4.51×10^{0}
^{264}Hs	10.59	1.1×10^{-3}	2.32×10^{-4}	3.98×10^{-4}
^{266}Hs	10.34	2.3×10^{-3}	9.96×10^{-4}	1.57×10^{-3}
^{270}Hs	9.020	2.2×10^{1}	8.01×10^{0}	7.72×10^{0}
^{270}Ds	11.20	1.0×10^{-4}	2.50×10^{-5}	4.76×10^{-5}
^{286}114	10.33	1.3×10^{-1}	6.81×10^{-2}	8.04×10^{-2}
^{288}114	10.09	8.0×10^{-1}	3.18×10^{-1}	3.44×10^{-1}
^{292}116	10.80	1.8×10^{-2}	1.32×10^{-2}	1.67×10^{-2}
^{294}118	11.81	8.90×10^{-4}	1.42×10^{-4}	2.27×10^{-4}

the factor from UDL [16] indicating good explanation of the data. We would like to mention here that our formulation (31) derived from the quantal phenomenon of resonance scattering, unlike UDL using three adjustable parameters, gives a minimum value of $\sigma = 0.453$ with the variation of a single radius parameter $r_c \approx 0.937$ fm which accounts for a physical quantity, namely the sum of the charge radii of the α and the daughter nuclei.

We can give an overall explanation of the data by presenting the data in graphical form of the variation of the quantity $\tau = \log_{10} T_{1/2} - b\zeta - h_{\log}$ as a function of χ (see eq. (32)). We take the experimental values of half-lives of α-decay of 390 nuclei consisting of elements with Z =52–120 and A =106–299 from ref. [15] and show them in the above form of variation τ vs. χ in figure 7 as solid circles. The results of $T_{1/2}^{\text{expt}}$ in this form of presentation aligned themselves in a linear fashion. The corresponding results from our calculation using formula (32) with an average value for $r_c = 0.923$ fm are shown by a solid curve in figure 7. It is seen that our results (solid curve) also show linear pattern and fall in the middle of the broader rectilinear arrangement of the data of 390 nuclei. This sort of presentation of the data of decay half-lives and their explanation are seen in [16, 18,19]. It may be pointed out here that the explanation of the data in this form, though decent looking, is not point to point comparison between the calculated and the experimental data as seen in the form of variation of $\log_{10} T_{1/2}$ as a function of neutron number N in figures 2–4.

We can apply the present formulation to the decay of a cluster ion from an exotic nucleus and estimate the decay half-life to compare with the corresponding experimental result. The experimental Q-values and the results of decay half-lives of different such decay events are obtained from ref. [21]. Using this Q-value and mass and charge numbers of the nucleus emitting the cluster in the formulae (32) with range R given by (40), we calculate $\log_{10} T_{1/2}$. These results of $T_{1/2}$ are presented by the quantity $\tau = \log_{10} T_{1/2} - b\zeta - h_{\log}$ as a function of χ in figure 8 as a solid curve and are compared with the corresponding experimental results (solid square) extracted from the measured values of $T_{1/2}$ from ref. [21]. In this case also, we achieve equally good explanation of the measured data with linear characteristic of variation of τ as a function of χ as observed in the analysis of α decay. In figure 9, the variation of the results of the quantity $\tau = \log_{10} T_{1/2} - b\zeta - h_{\log}$ with χ in both α and cluster decays using global range R (40) are presented together. It is seen that both of them fall on a single straight path with a common value of slope and

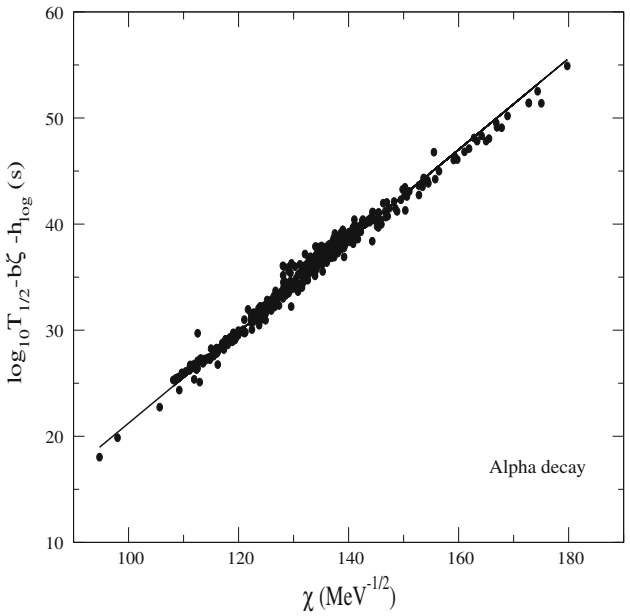

Figure 7. Plot of decay law (32) for α-decays in $\ell = 0$ state from 390 number of nuclei with $Z = 52$–120. The straight line is given as $\chi + c$ of eq. (32). Solid circles represent experimental data from ref. [15].

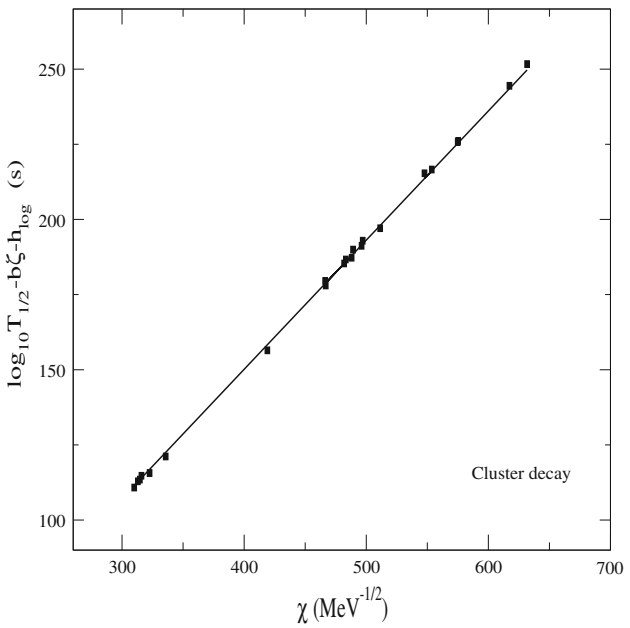

Figure 8. Same as figure 7 for decays of cluster ions. Solid squares represent experimental data from ref. [21].

intercept. This manifestation makes the nature of the present formulation of decay rate broad and universal showing no discrimination amongst the events of emission of positively charged clusters of different Z values emerging out from metastable parent nuclei with charge number ranging from small $Z = 52$ to Z as large as 120 in the superheavy region of the nuclei.

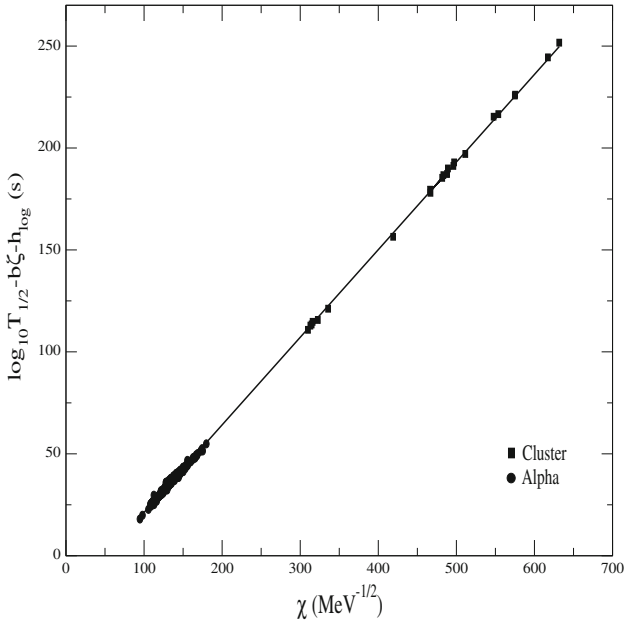

Figure 9. Same as figure 7 for decays of α and cluster ions together.

4. Summary and conclusion

The emission of α-particle from a parent nucleus is understood as a two-body quantum collision phenomenon involving the daughter and the parent nuclei. The true interaction between α and daughter nucleus is approximated by the combination of a Dirac δ well and repulsive Coulomb potentials. Resonances are generated by this δ well decorated Coulomb potential based on the principle that the presence of a reflecting barrier potential entails a destabilisation of the bound state of the Dirac δ potential well and generates resonance (quasistationary) states. The energy derivative of the phase-shift of the S-matrix of the transition scattering from an isolated quasibound state to a scattering state is related to the width (Γ) of the resonance and hence the half-life $T_{1/2} = \ln 2\hbar/\Gamma$ of α-decay.

Using exact solutions of the delta well driven Coulomb potential, we derive a compact expression for $\log_{10} T_{1/2}$ in terms of Q-value and the mass and charge numbers of the α emitter with a radius parameter specifying the size of the emitter.

By fitting the experimental results of α-decay half-lives of a large number of nuclei individually by the calculated values of half-lives with the variation of the range parameter r_c of the formula, we find a nearly constant value of $r_c \approx 0.93$ fm for different nuclei. The result of the range $R = r_c(A_\alpha^{1/3} + A_d^{1/3})$ with $r_c = 0.93$ fm gives information about the sum of the charge radii of the participants, α and daughter nucleus.

Using the above average result of R or the global expression for sharp radius of the parent nucleus, the expression of $\log_{10} T_{1/2}$ is computed with Q-values for α decay obtained from a mass table. These computed results successfully explain the experimental results of α-decay half-lives ranging from 10^{-7}s to 10^{25}s in the cases of many light, heavy and superheavy radioactive nuclei with charge number $Z = 52$–120 and mass number $A = 106$–299.

Having uniformly applied the formulation to the decays of α as well as cluster ions, the universal or global nature of the decay rule is established.

In conclusion, an expression for decay half-life of positive ion is derived from the phase-shift of transition scattering from an isolated quasibound state to a scattering state. Taking only the Q-value and the mass and charge numbers of the emitter from a mass table and adjusting a single radius parameter akin to the size of the emitter, one can explain as well as predict the results of the decay half-lives of cluster ions of any charge numbers including α-particle.

References

[1] S Aberg, P B Semmes and W Nazarewicz, *Phys. Rev. C* **56**, 1762 (1997)

[2] H Feshbach, *Theoretical nuclear physics: Nuclear reactions* (Wiley, New York, 1992)

[3] S G Kadmenskii and V E Kalechtis, *Sov. J. Nucl. Phys.* **12**, 37 (1971)

[4] G R Satchler, *Direct nuclear reactions* (Oxford University Press, New York, 1983)

[5] N K Glendenning, *Direct nuclear reactions* (Academic, New York, 1983)

[6] Claude Aslangul, *Am. J. Phys.* **63**, 935 (1995)

[7] E P Wigner, *Phys. Rev.* **98**, 145 (1955)

[8] V D Mur and V S Popov, *Theor. Math. Phys.* **65**, 1132 (1985)

[9] V D Mur, B M Karnakov, S G Pozdnyakov and V S Popov, *Phys. At. Nucl.* **56**, 217 (1993)

[10] L P Kok, J W de Maag, H H Brouwer and H van Haeringen, *Phys. Rev. C* **26**, 2381 (1982)

[11] Benjamin K Luna and T Papenbrock, *Phys. Rev. C* **100**, 054307 (2019)

[12] M Abramowitz and I A Stegun, *Handbook of mathematical functions with formulas, graphs, and mathematical tables* (Dover Publications, Inc., New York, 1965)

[13] J Blocki, J Randrup, W J Swiatecki and C F Tsang, *Ann. Phys. (NY)* **105**, 427 (1977)

[14] M Wang *et al*, *Chin. Phys.* **36**, 1603 (2012)

[15] M Ismail, A Y Ellithi, M M Selim, N Abou-Samra and O A Mohamedien, *J. Phys. G: Nucl. Part. Phys.* **47**, 055105 (2020)

[16] C Qi, F R Xu, R J Liotta and R Wyss, *Phys. Rev. Lett.* **103**, 072501 (2009)

[17] J C Pei, F R Xu, Z J Lin and E G Zhao, *Phys. Rev. C* **76**, 044326 (2007)

[18] Basudeb Sahu and Swagatika Bhoi, *Phys. Rev. C* **93**, 044301 (2016)

[19] B Sahu, R Paira and B Rath, *Nucl. Phys. A* **908**, 40 (2013)

[20] K P Santhosh and C Nithya, *Phys. Rev. C* **95**, 054621 (2017)

[21] Yibin Qian and Zhongzhou Ren, *J. Phys. G: Nucl. Part. Phys.* **39**, 015103 (2012)